

Supplementary Material for

Characterisation of NO production and consumption: New insights by an improved laboratory dynamic chamber technique

T. Behrendt¹, P. R. Veres², F. Ashuri¹, G. Song^{1,3}, M. Flanz⁴, B. Mamtimin¹, M. Bruse⁵, J. Williams⁴ and F.X. Meixner¹

[1]{Biogeochemistry Department, Max Planck Institute for Chemistry, Mainz, Germany}

[2]{Now at Cooperative Institute for Research in Environmental Sciences, Boulder, CO 80305, USA}

[3] {Institute of Applied Ecology, Chinese Academy of Sciences, Shenyang, P.R. China}

[4] {Atmospheric Chemistry Department, Max Planck Institute for Chemistry, Mainz, Germany}

[5]{Environmental Modelling Group (EMG), Johannes Gutenberg University Mainz, Mainz, Germany}

*Correspondence to: T. Behrendt (thomas.behrendt@mpic.de)

1 **S1. Determination of soil sample's moisture from measurements of water vapour in the**
 2 **headspace of the laboratory dynamic chamber - a mass balance approach**

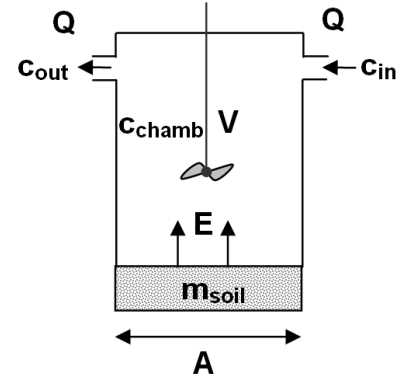
3 Considering the H₂O vapour mass flux, i.e. the derivative of M_{H_2O} with respect to time
 4 ($\partial M_{H_2O}/\partial t = \Phi_{H_2O}$ in kg s⁻¹), the individual flux components of the laboratory dynamic
 5 chamber system are defined as

6
 7 $\Phi_{in} =$ mass flux of H₂O into chamber: $Q \cdot c_{H_2O,in}$

8 $\Phi_{out} =$ mass flux of H₂O out of chamber: $Q \cdot c_{H_2O,out}$

9 $\Phi_{soil} =$ mass flux of H₂O due to evaporation E

10 from soil: $A \cdot E$



11
 12 where $c_{H_2O,in}$, $c_{H_2O,out}$, and $c_{H_2O,cham}$ are H₂O vapor concentrations (in kg m⁻³, i.e. absolute
 13 humidity) at the inlet, the outlet and within the dynamic chamber; Q is the purging rate (m³ s⁻¹),
 14 A is the cross section (m²), and V is the volume (m³) of the dynamic chamber. E is the flux
 15 density of H₂O vapour due to evaporation from the soil sample (kg m⁻² s⁻¹), and m_{soil} is the
 16 (total) mass of the soil sample in kg ($m_{soil} = m_{soil,dry} + m_{soil,water}$). Furthermore, there are two
 17 well accepted prerequisites (c.f., Pape et al., 2009): (a) $c_{H_2O,cham} = c_{H_2O,out}$ (due to the effective
 18 mixing of the headspace's air by the fan and the high purging rate Q (i.e., short exchange time
 19 τ of the chamber's headspace volume), and (b) the H₂O vapour mass flux from the soil
 20 sample ($A \cdot E$) is equal to the temporal change of the total soil mass ($dm_{soil}(t)/dt$).

21 The dynamic chamber's mass balance of the H₂O vapour mass flux is then given by:

22
$$V \frac{dc_{H_2O,cham}(t)}{dt} = Q c_{H_2O,in}(t) - Q c_{H_2O,cham}(t) + \frac{dm_{soil}(t)}{dt} \quad (S1)$$

23 For the sake of convenience, data of H₂O vapor are considered only in terms of the measured
 24 signal s (in arbitrary units), where the relation between s and the H₂O vapour concentration is
 25 given by $c(t) = g \cdot s(t)$. Then, Eq. (S1) reads as follows:

26
$$V g \frac{ds_{H_2O,cham}(t)}{dt} = g Q s_{H_2O,in}(t) - g Q s_{H_2O,cham}(t) + \frac{dm_{soil}(t)}{dt} \quad (S1.1)$$

1 For each experiment, the total soil mass is determined (weighing) at the begin ($t = t_0$) and the
 2 end ($t = t_s$), as well as $s_{H_2O,in}(t_0)$, $s_{H_2O,in}(t_s)$, $s_{H_2O,cham}(t_0)$, and $s_{H_2O,cham}(t_s)$. Furthermore, we
 3 assume, that within a sufficiently short time interval, namely between t_i and t_{i-1} , the temporal
 4 change of $s_{H_2O,cham}(t)$ and $s_{H_2O,in}(t)$ is linear, i.e.,

$$5 \quad s_{H_2O,in}\left(\frac{t_{i-1} + t_i}{2}\right) = \frac{s_{H_2O,in}(t_{i-1}) + s_{H_2O,in}(t_i)}{2} \quad (S2.1)$$

$$6 \quad s_{H_2O,cham}\left(\frac{t_{i-1} + t_i}{2}\right) = \frac{s_{H_2O,cham}(t_{i-1}) + s_{H_2O,cham}(t_i)}{2} \quad (S2.2)$$

7 Re-arranging of Eq. (S1) gives :

$$8 \quad \frac{dm_{soil}(t)}{dt} = g Q s_{H_2O,cham}(t) - g Q s_{H_2O,in}(t) + V g \frac{ds_{H_2O,cham}(t)}{dt} \quad (S1.2)$$

9 Integration of both sides of Eq.(S1.2) with respect to t_0 and t_s :

$$10 \quad \int_{t_0}^{t_s} \frac{dm_{soil}(t)}{dt} dt = g Q \int_{t_0}^{t_s} s_{H_2O,cham}(t) dt - g Q \int_{t_0}^{t_s} s_{H_2O,in}(t) dt + V g \int_{t_0}^{t_s} \frac{ds_{H_2O,cham}(t)}{dt} dt \quad (S3)$$

11 This is equivalent to:

$$12 \quad m_{soil}(t_s) - m_{soil}(t_0) = V g [s_{H_2O,cham}(t_s) - s_{H_2O,cham}(t_0)] + \\ 13 \quad + g Q \int_{t_0}^{t_s} s_{H_2O,cham}(t) dt - g Q \int_{t_0}^{t_s} s_{H_2O,in}(t) dt \quad (S3.1)$$

14 Considering individual time sub-intervals (t_i ; t_{i-1}), then both integrals of Eq. (S3.1) can be
 15 written as:

$$16 \quad \int_{t_0}^{t_s} s_{H_2O,cham}(t) dt = \sum_{i=1}^{i=S} \int_{t_{i-1}}^{t_i} s_{H_2O,cham}(t) dt \quad (S4.1)$$

$$17 \quad \int_{t_0}^{t_s} s_{H_2O,in}(t) dt = \sum_{i=1}^{i=S} \int_{t_{i-1}}^{t_i} s_{H_2O,in}(t) dt \quad (S4.2)$$

18 Making use of the “mean value theorem of integral calculus”, and assuming that (a)
 19 $s_{H_2O,cham}(t)$ and $s_{H_2O,in}(t)$ are between t_i and t_{i-1} sufficiently well approximated by linear
 20 representation, (b) $t_i - t_{i-1}$ is sufficiently small, then:

$$1 \quad \int_{t_{i-1}}^{t_i} s_{H_2O, cham}(t) dt = (t_i - t_{i-1}) \frac{s_{H_2O, cham}(t_i) + s_{H_2O, cham}(t_{i-1})}{2} \quad (S5.1)$$

$$2 \quad \int_{t_{i-1}}^{t_i} s_{H_2O, in}(t) dt = (t_i - t_{i-1}) \frac{s_{H_2O, in}(t_i) + s_{H_2O, in}(t_{i-1})}{2} \quad (S5.2)$$

3 Combining Eqs. (S4.1), (S4.2), (S5.1), (S5.2) with Eq. (S3.1) leads to:

$$4 \quad m_{soil}(t_S) - m_{soil}(t_0) = g \left(V [s_{H_2O, cham}(t_S) - s_{H_2O, in}(t_0)] + S_0 \right) \quad (S3.2)$$

5 where

$$6 \quad S_0 = Q \left(\sum_{i=1}^{i=S} (t_i - t_{i-1}) \frac{s_{H_2O, cham}(t_i) + s_{H_2O, cham}(t_{i-1})}{2} - \sum_{i=1}^{i=S} (t_i - t_{i-1}) \frac{s_{H_2O, in}(t_i) + s_{H_2O, in}(t_{i-1})}{2} \right) \quad (S3.3)$$

7 which is equivalent to

$$8 \quad S_0 = Q \left(\sum_{i=1}^{i=S+1} (T_i + T_{i-1}) [s_{H_2O, cham}(t_{i-1}) - s_{H_2O, in}(t_{i-1})] \right); \quad T_i = \frac{t_i - t_{i-1}}{2}; \quad T_0 = T_{S+1} = 0 \quad (S3.4)$$

9 Re-arranging Eq. (S3.2) provides the formula to determine the proportionality factor g of
10 $c(t)$ and $s(t)$:

$$11 \quad g = \frac{m_{soil}(t_S) - m_{soil}(t_0)}{V [s_{H_2O, cham}(t_S) - s_{H_2O, in}(t_0)] + S_0} \quad (S6)$$

12 which includes the ‘‘calibration’’ of the integrated, arbitrary H₂O vapour signal by the amount
13 of evaporated soil water which has been simply determined by weighing the soil sample
14 before and after the experiment.

15 With the knowledge of g , a recursion formula for the calculation of the actual soil mass (and
16 hence the actual soil moisture) is developed from Eq. (S3.2). Considering individual time sub-
17 intervals $(t_i; t_{i-1})$ instead of $(t_0; t_S)$, Eq. (S3.1) can be formulated as:

$$18$$

$$19 \quad m_{soil}(t_i) - m_{soil}(t_{i-1}) = V g [s_{H_2O, cham}(t_i) - s_{H_2O, in}(t_{i-1})] +$$

$$20 \quad + g Q \int_{t_{i-1}}^{t_i} s_{H_2O, cham}(t) dt - g Q \int_{t_{i-1}}^{t_i} s_{H_2O, in}(t) dt \quad (S7)$$

21 Considering Eqs. (S5.1) and (S5.2), and resolving Eq. (S7) for $m_{soil}(t_i)$ provides the desired re-
22 cursion formula for calculation of $m_{soil}(t_i)$:

$$1 \quad m_{soil}(t_i) = m_{soil}(t_{i-1}) + V g [s_{H_2O, cham}(t_i) - s_{H_2O, cham}(t_{i-1})] + S_i \quad (S7.2)$$

2 where

$$3 \quad S_i = (T_i + T_{i-1}) [s_{H_2O, cham}(t_{i-1}) - s_{H_2O, in}(t_{i-1})]; \quad T_i = \frac{t_i - t_{i-1}}{2}; \quad T_0 = T_{S+1} = 0 \quad (S7.3)$$

4

5 **S2. Standard deviation of the proportionality factor g , actual total soil mass $m_{soil}(t_i)$, and** 6 **actual gravimetric soil moisture $\theta_g(t_i)$**

7 To calculate σ_g , Eq. (S6) and Eq. (S3.4) are recalled:

$$8 \quad g = \frac{m_{soil}(t_S) - m_{soil}(t_0)}{V [s_{H_2O, cham}(t_S) - s_{H_2O, cham}(t_0)] + S_0} \quad (S6)$$

$$9 \quad S_0 = Q \left(\sum_{i=1}^{i=S+1} (T_i + T_{i-1}) [s_{H_2O, cham}(t_{i-1}) - s_{H_2O, in}(t_{i-1})] \right); \quad T_i = \frac{t_i - t_{i-1}}{2}; \quad T_0 = T_{S+1} = 0 \quad (S3.4)$$

10 Consequently, the derivatives of g with respect to $m_{soil}(t_0)$, $m_{soil}(t_S)$, V , $s_{H_2O, cham}(t_0)$,
11 $s_{H_2O, cham}(t_S)$, Q , and S_0 , as well as their standard deviations ($\sigma_{m_{soil}(t_0)}$, $\sigma_{m_{soil}(t_S)}$, σ_V , $\sigma_{s_{cham}(t_0)}$,
12 $\sigma_{s_{cham}(t_S)}$, σ_Q , and σ_{S_0}) have to be considered. Application of general Gaussian error
13 propagation leads to:

$$14 \quad \sigma_g = \pm \left(\frac{\Delta m}{D^2} \right) \left[\left(\frac{D}{\Delta m} \right)^2 (\sigma_{m_{soil}(t_S)}^2 + \sigma_{m_{soil}(t_0)}^2) + (-\Delta s \sigma_V)^2 + V^2 (\sigma_{s_{cham}(t_S)}^2 + \sigma_{s_{cham}(t_0)}^2) + \sigma_{S_0}^2 \right]^{\frac{1}{2}} \quad (S8)$$

15 where

$$16 \quad D = V \Delta s + S_0 \quad (S8.1)$$

$$17 \quad \Delta m = m_{soil}(t_S) - m_{soil}(t_0) \quad (S8.2)$$

$$18 \quad \Delta s = s_{H_2O, cham}(t_S) - s_{H_2O, cham}(t_0) \quad (S8.3)$$

$$19 \quad \sigma_{S_0}^2 = \left(\sigma_Q \frac{S_0}{Q} \right)^2 + Q^2 \sum_{i=1}^{i=S+1} (T_i + T_{i-1})^2 [\sigma_{s_{cham}(ti-1)}^2 + \sigma_{s_{in}(ti-1)}^2]; \quad T_i = \frac{t_i - t_{i-1}}{2}; \quad T_0 = T_{S+1} = 0 \quad (S8.4)$$

20 Here – for the sake of simplicity – the most simple formulation of Eq. (S8.4) is given, which
21 is only valid for $\sigma_{s_{cham}(ti)} = \sigma_{s_{cham}(ti-1)} = \sigma_{s_{in}(ti)} = \sigma_{s_{in}(ti-1)} = \sigma_s = \text{const.}$ (as shown by experi-

1 mental evidence). If $\sigma_{s\text{cham}(ti)} \neq \sigma_{s\text{cham}(ti-1)} \neq \sigma_{s\text{in}(ti)} = \sigma_{s\text{in}(ti-1)} \neq \sigma_s \neq \text{const.}$, σ_{s0} can still be
 2 formulated in full, but becomes more complex. Since σ_V and σ_Q are usually negligible (1% of
 3 V and Q , respectively), $\sigma_{m\text{soil}(t0)}$, $\sigma_{m\text{soil}(tS)}$, $\sigma_{s\text{cham}(t0)}$, and $\sigma_{s\text{cham}(tS)}$ are known from
 4 corresponding measurements, Eqs. (S8) and (S8.4) read as follows:

$$5 \quad \sigma_g = \pm \left(\frac{\Delta m}{D^2} \right) \left[\left(\frac{D}{\Delta m} \right)^2 (\sigma_{m\text{soil}(tS)}^2 + \sigma_{m\text{soil}(t0)}^2) + V^2 (\sigma_{s\text{cham}(tS)}^2 + \sigma_{s\text{cham}(t0)}^2) + \sigma_{s0}^2 \right]^{\frac{1}{2}} \quad (\text{S9})$$

$$6 \quad \sigma_{s0}^2 = 2 \sigma_s^2 Q^2 \sum_{i=1}^{i=S+1} (T_i + T_{i-1})^2; \quad T_i = \frac{t_i - t_{i-1}}{2}; \quad T_0 = T_{S+1} = 0 \quad (\text{S9.1})$$

7 To calculate the standard deviation $\sigma_{m\text{soil}(ti)}$ of the actual total soil mass $m_{\text{soil}(ti)}$, Eqs. (S7.2)
 8 and (S7.3) are recalled:

$$9 \quad m_{\text{soil}(t_i)} = m_{\text{soil}(t_{i-1})} + V g [s_{H2O,\text{cham}}(t_i) - s_{H2O,\text{cham}}(t_{i-1})] + S_i \quad (\text{S7.2})$$

$$10 \quad S_i = (T_i + T_{i-1}) [s_{H2O,\text{cham}}(t_{i-1}) - s_{H2O,\text{in}}(t_{i-1})]; \quad T_i = \frac{t_i - t_{i-1}}{2}; \quad T_0 = T_{S+1} = 0 \quad (\text{S7.3})$$

11 The most simple formulation for $\sigma_{m\text{soil}(ti)}$ is derived for negligible σ_V and σ_Q and for $\sigma_{s\text{cham}(ti)}$
 12 $= \sigma_{s\text{cham}(ti-1)} = \sigma_{s\text{in}(ti)} = \sigma_{s\text{in}(ti-1)} = \sigma_s = \text{const.}$ (see above), namely

$$13 \quad \sigma_{m\text{soil}(ti)} = \pm \left[\sigma_{m\text{soil}(ti-1)}^2 + \left[\sigma_g V (s_{\text{cham}}(t_i)(1 + QT_i) - s_{\text{cham}}(t_{i-1})(1 - QT_i) - \right. \right. \\ 14 \quad \left. \left. - QT_i (s_{\text{in}}(t_i) + s_{\text{in}}(t_{i-1})) \right) \right]^2 + 2 \sigma_s^2 g^2 ((V + QT_i)^2 + Q^2 T_i^2) \right]^{\frac{1}{2}} \quad (\text{10})$$

15 As already mentioned above for σ_{s0} , if $\sigma_V \neq 0$, $\sigma_Q \neq 0$ and $\sigma_s \neq \text{const.}$, the formulation for σ_m
 16 $\text{soil}(ti)$ can still be written in full, but becomes more complex.

17 The dimensionless gravimetric soil moisture is defined by $\theta_g = (m_{\text{soil,wet}} - m_{\text{soil,dry}})/m_{\text{soil,dry}}$.
 18 During the entire period of drying-out a soil sample in the laboratory dynamic chamber, the
 19 actual gravimetric soil moisture $\theta_g(t_i)$ is then given by

$$20 \quad \theta_g(t_i) = \frac{m_{\text{soil}}(t_i) - m_{\text{soil}}(t_S)}{m_{\text{soil}}(t_S)} \quad (\text{S11})$$

21 where $m_{\text{soil}}(t_S)$ is the mass of the soil sample at the end ($t = t_S$) of each laboratory drying-out
 22 experiment (determined by weighing). Application of Gaussian error propagation calculus to
 23 Eq. (11) delivers for $\sigma_{\theta_g(ti)}$,

$$\sigma_{\theta_{g(i)}} = \pm \left[\left(\frac{\sigma_{m_{soil}(t_i)}}{m_{soil}(t_S)} \right)^2 + \left(-\frac{m_{soil}(t_i)}{m_{soil}^2(t_S)} \sigma_{m_{soil}(t_S)} \right)^2 \right]^{\frac{1}{2}} \quad (S12)$$

2

3 **S3. Control and automatic adjustment of incubation conditions**

4 S3.1 Control of incubation conditions

5 A scheme of the control of the improved laboratory dynamic chamber system is shown Figure
6 S1. The control routine starts at the lower of the selected soil temperatures; then humidificati-
7 on and the lower of the selected NO mixing ratios of the flushing air stream are adjusted for
8 the “Meas low” and the “Flush flow” (Fig. S2). Next, the control scheme checks whether the
9 system’s temperature, the relative humidity, and the NO mixing ratio of the flushing air
10 stream fulfil pre-scribed stability criteria, namely ± 0.2 K, ± 3 %, and < 1 ppb (low NO mixing
11 ratio; < 2 % in case of higher NO mixing ratio), respectively. Then the gas stream is
12 sequentially cycled through all chambers, where the cycle serving box0 to box6 is called the
13 “box cycle”, and the cycle, which switches between low and high NO mixing ratio, is called
14 the “NO cycle”. Having completed a “box cycle” at low NO mixing ratio, the control scheme
15 adjusts for the higher NO mixing ratio (usually 133 ppb). During the adjustment period, two
16 gas streams are simultaneously probed. That gas stream, where NO mixing ratio is actually
17 increasing is directed through the reference chamber (so-called “incoming air”) and be
18 measured by the NO-analyzer after the stability criterion ($\pm 2\%$ of prescribed mixing ratio) is
19 reached. During this stabilization period, soil chambers are switched into the static mode to
20 enable determination of the net CO₂ release through the measurement of the temporal increase
21 of the CO₂ mixing ratio (see Fig. S3). It has to be noted that the CO₂ measurement starts after
22 NO mixing ratio is already constant (t_{63} is 3 minutes for equilibration chambers’ headspace
23 NO mixing ratio within $< \pm 1$ ppb). Control of the adjustment of NO mixing ratio and feed-
24 back observation of the stability criterion leads to that level of NO mixing ratio’s temporal
25 stability which is essential for the high precision NO measurements requested in this study.
26 This is particularly important for the switch back to the lower of the two selected NO mixing
27 ratios (usually “zero”-air). For practical reasons (temporal constraint for the entire drying-out
28 experiment), it was decided to probe only three soil chambers in the static mode (4 minutes
29 each) during one individual period of NO mixing ratio adjustment. The remainder of six soil

1 chambers is immediately probed after the “box cycle” is completed, and the next NO mixing
2 ratio will be adjusted as part of the “NO cycle”. Now the system’s temperature is switched to
3 the next higher/lower level accompanied by corresponding adjustment of the relative
4 humidity of the flushing air stream. It needs 28 minutes (t_{63}) to adjust the system’s tempera-
5 ture (hence, soil temperature) and 2 minutes (t_{63}) for relative humidity. Another 10-15
6 minutes are allowed for satisfying corresponding stability criteria (i.e., ± 0.2 K and ± 3 %, re-
7 spectively). Now, the “box cycle” at the lower NO mixing ratio level starts: three soil
8 chambers (in static mode) are probed for CO₂ mixing ratio during the adjustment period of
9 “incoming air” NO mixing ratio, and after its stabilization all six chambers (switched back to
10 dynamic mode) are sequentially probed for each chamber’s headspace NO mixing ratio. Then,
11 as part of the “NO cycle”, the control scheme switches to higher NO mixing ratio, chambers
12 are switched to the static mode, the remainder of 6 chambers are probed for CO₂ mixing ratio
13 during the adjustment period of the higher “incoming air” NO mixing ratio, chambers are
14 switched to the dynamic mode, another “box cycle” will be completed before the control
15 scheme switches the system’s temperature to the next lower/higher level. Finally, switching
16 and cycling procedures are repeated until the soil is completely dried out.

17 For the sake of completeness, it should be noted that (i) the total time for drying-out can be
18 extended by humidifying the air of the “Meas flow” as well as the “Flush flow”, (ii) response
19 time (t_{63}) of the CO₂/H₂O-analyzer is < 10 s, and (iii) t_{63} of the NO-analyzer is 90 s. These
20 response times are very small compared to those time periods which are necessary to switch
21 and stabilize the incubation condition of the improved laboratory dynamic chamber system (s.
22 above). Nevertheless, to eliminate any potential memory effects, which might be due the
23 sequential switching from one chamber to another, only the last 90 s of data from the entire
24 probing period (240 s) of each chamber are kept for further evaluation.

25

26 S3.2 Details of system’s temperature (soil temperature) control

27 The soil sample enclosed in the soil chamber can be characterized as a system of considerable
28 thermal inertia, i.e., fast changes of system’s temperature (which is the air temperature inside
29 the thermostat cabinet) will hardly impact the temperature of the soil sample. This is very for-
30 tunate for the investigation release rates at constant temperature, but once the soil temperature
31 should be changed to another (pre-scribed) level, it will take a large amount of (heating/cool-

1 ing) energy and a long time until the system will be stable again. Therefore, a time discrete PI
2 controller with an update rate of 5Hz was used to regulate the soil temperature in the im-
3 proved laboratory dynamic chamber system. In general, a PI controller is comparing the dif-
4 ference of a constant set value and a changing input. In the incubation system the PI controller
5 is a software based calculation of that difference which is divided into a proportional and inte-
6 gral part. The higher the proportional part, the faster reacts the controller but the higher the
7 chance to result oscillations. Therefore, the integral part is used to compensate for oscillations
8 by small changes in the output. In a first test experiment the air temperature of the thermostat
9 cabinet was used as input temperature for the PI controller. This result a delay of the system
10 of approximately 20 hours until the soil temperature was in equilibrium with the 10 K
11 increased air temperature. The soil temperature itself could not be used as input temperature
12 since the inertia of the system leads to even longer time constants. To accelerate fast
13 temperature switching, the discrete set value of the PI controller was replaced by continuously
14 changing soil temperature as

$$15 \quad SetValue_{PI,T} = (R_T \cdot (Set_{T_{soil}} - T_{soil})) + Set_{T_{soil}} \quad (S13)$$

16 where $Set_{T_{soil}}$ is the set soil temperature (in °C; usually either 20°C or 30°C), T_{soil} the actual
17 soil temperature (in °C), and R_T a system dependent, dimensionless factor to raise the set
18 point (usually between 2 and 3). The adjustment of the soil temperature for an increase from
19 20 to 30°C is shown in Figure S4 to demonstrate the use R_T to raise the set point. When the
20 routine is started, the lower soil temperature, the humidification and the “incoming air” NO
21 mixing ratio are adjusted. The soil temperature is an average of the two chambers in the centre
22 of the thermostat cabinet. Similar to Gödde and Conrad (1999) different temperature switches
23 of 5 and 10°C were tested. The present version of the improved laboratory dynamic chamber
24 system needs approx. 40–50 minutes to adjust soil temperatures for an increase or decrease of
25 10 K.

26 Since there were no significant differences between 5 K and 10 K switches, the 10 K switch
27 has been chosen (from 20°C to 30°C). Since the total time of drying-out is limited, it is not
28 recommended to switch more than two different NO mixing ratios and soil temperatures
29 within one drying-out experiment.

30

31 S3.3 Details of relative humidity control of the flushing air stream

1 As for soil temperature, the relative humidity of the “Meas flow” and “Flush flow” is
2 controlled by a PI-controller as well. However, it has to be noted, that through humidification
3 of these air flows, drying-out of soil samples could not be completely stopped, but slowed
4 down considerably. Since each soil of the enclosed sample is characterized by different field
5 capacity and drying-out behaviour over time, several tests resulted in a time dependent look-
6 up function for the control of humidification. This function could be used for all kinds of
7 soils. Basically, for the total time of a drying-out experiment, a table consisting of 20 time
8 increments is programmed, where for the first 14 increments the humidification is constant at
9 95% relative humidity and the last 6 increments the humidification is linearly decreasing to
10 0%. Once, the time for drying-out of a soil sample is known (usually about 1 day for desert
11 soil and up to 5 days for organic rich soils), the set value for the humidification is the result of
12 the interpolation of the relative humidity between the time increments which depend on the
13 time of measurement and that for the total drying-out experiment. Input data for control of the
14 relative humidity are measured data obtained by a digital humidity probe HTM B71 (HY-
15 LINE SENSOR-TEC, Germany) mounted in the headspace of the reference (empty) soil
16 chamber. The relative humidity of the “Meas flow” and “Flush flow” is then controlled by
17 mixing dry and wet air flows together (s. Figs. S1–S3). The control scheme of the improved
18 laboratory dynamic chamber system is programmed such, that flexible experimental perfor-
19 mance is possible (considering other incubation conditions then chosen here): before starting
20 the control scheme, incubation conditions (“incoming air” NO mixing ratio switch, static
21 mode switch, soil temperature switch, humidification switch) may be (independently from
22 each other) pre-scribed interactively.
23

1
2
3
4
5
6
7
8
9
10
11
12
13
14
15
16
17
18
19
20
21
22
23
24
25
26
27
28
29

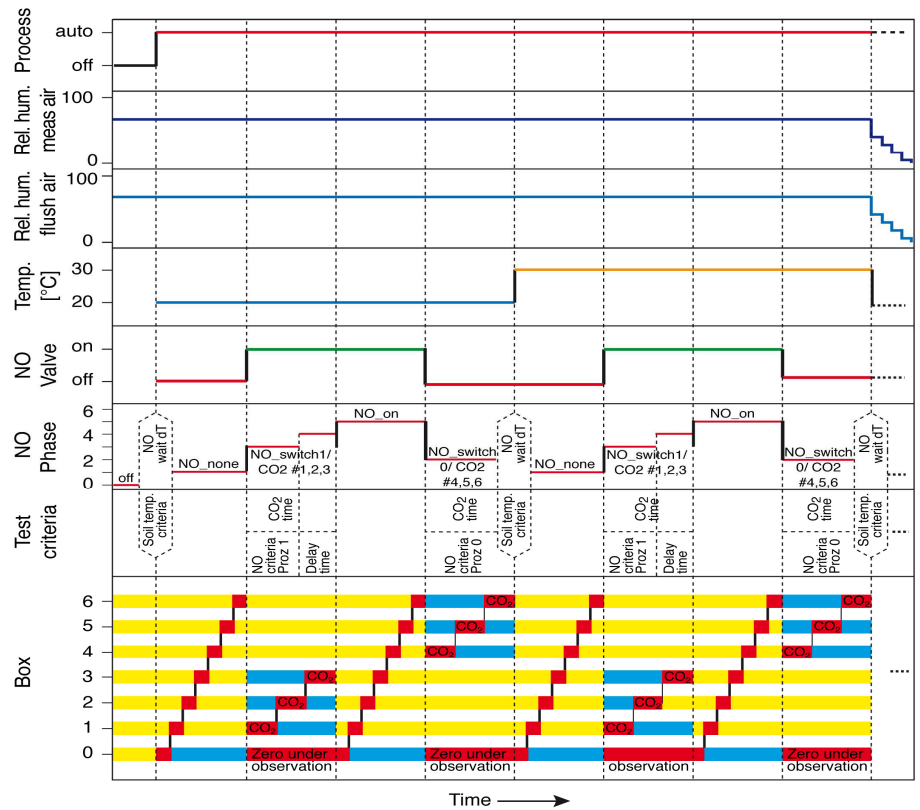


Fig. S1: Scheme for automatic control of the improved laboratory dynamic soil chamber system, NO headspace concentration, CO₂ mode, soil temperature and humidification

1
2
3
4
5
6
7
8
9
10
11
12
13
14
15
16
17
18
19
20
21
22
23
24
25

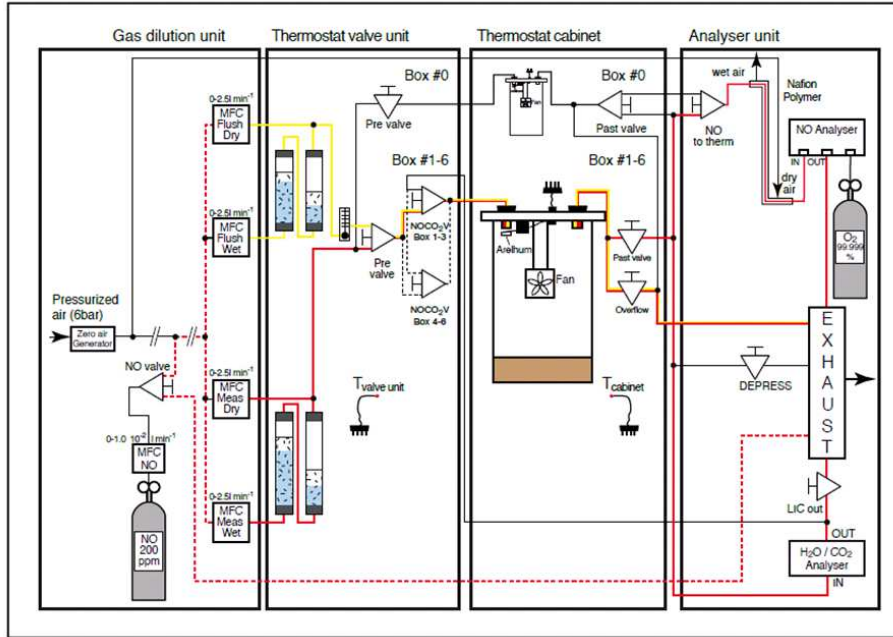


Fig. S2: Gas flow for the valve switch for the NO headspace concentration (red dots), the separate humidified Meas flow (red) and humidified Flush flow (yellow) for the not measured chambers in dynamic chamber mode to analyse NO

1
2
3
4
5
6
7
8
9
10
11
12
13
14
15
16
17
18
19
20
21
22
23
24
25

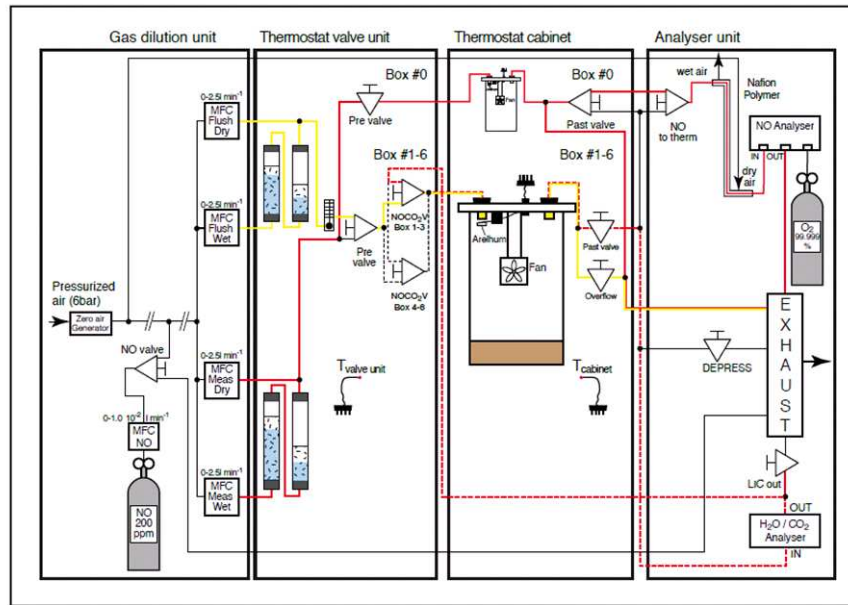


Fig. S3: Gas flow for the valve switch for CO₂ measurement (red dots), the switch of the bypass mode for observation of NO (red) and humidified Flush flow (yellow) for the not measured chambers in the static chamber mode to analyse CO₂

1
2
3
4
5
6
7
8
9
10
11
12
13
14
15
16
17
18
19

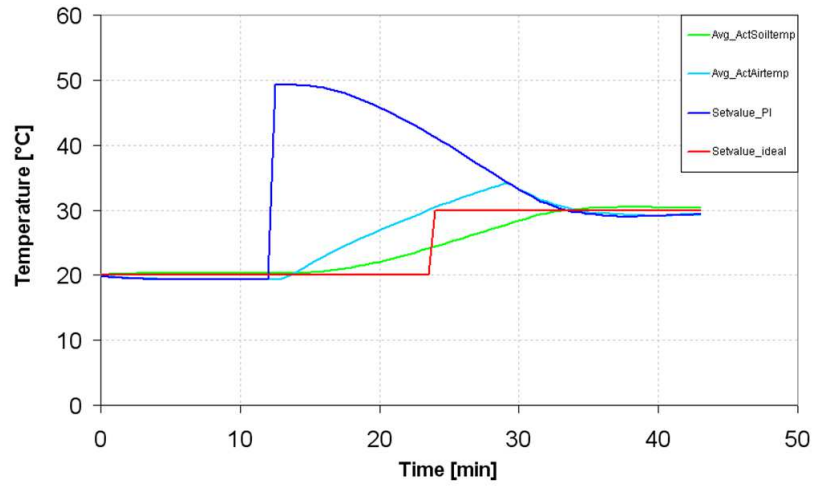


Fig. S-4: Example of the transient response of the soil temperature during a 10 K temperature change (from $T_{\text{soil}}=20^{\circ}\text{C}$ to $T_{\text{soil}}=30^{\circ}\text{C}$).